Faculty of Mathematical Sciences

University of Twente

University for Technical and Social Sciences

P.O. Box 217
7500 AE Enschede
The Netherlands
Phone: +31-53-4893400
Fax: +31-53-4893114
Email: memo@math.utwente.nl

Memorandum No. 1495

Cross-sectional river shapes: A variational discharge-resistance formulation

P. Roos, F.P.H. van Beckum
and E.W.C. van Groesen

August 1999

ISSN 0169-2690

Cross-sectional river shapes: a variational discharge-resistance formulation

Pieter Roos*, Frits van Beckum and Brenny van Groesen
Faculty of Mathematical Sciences, University of Twente, Enschede, The Netherlands

August 23, 1999

Abstract

Cross-sectional river shapes were obtained from a variational principle: minimizing the bed friction for a given discharge and a given maximum lateral bed slope (angle of repose). The optimal shape is found to be independent of both the exponent in the friction law adopted and the value of the discharge, but it does depend on the angle of repose. The optimal profile is a single stream; for braided rivers the solution is suboptimal.

Keywords[1]

river cross-sections, river morphology, sediment transport, variational techniques

Introduction

A considerable part of the research in river morphology is aimed at obtaining a better understanding of dynamical phenomena like meandering and braiding. The commonly adopted model is direct in the sense that it directly describes the mechanisms involved. It contains depth-averaged flow equations, a sediment balance and a sediment transport formula. The latter one, describing the interaction between the flow and the mobile bed material, acts as closure for the model. The model usually allows for a basic state around which a stability analysis can be carried out.

*email: prooster@hotmail.com

[1]Mathematics Subject Classification: 86A05 (hydrology, hydrography, oceanography)

For example, Schielen *et al.* [7] consider an erodible bed between non-erodible vertical banks. As a result of this rather simple geometry, the basic state is easily found: a unidirectional flow above a fully horizontal bed. The stability analysis describes the growth pattern of morphological features at the bed. However, as the banks remain fixed, this approach cannot really describe the onset of meandering.

Therefore, the next step towards describing natural rivers rather than channels would be to drop the assumption of the somewhat artificial non-erodible banks. Hence, no distinction is made between bed and banks and the (erodible) banks will emerge naturally as a result of the rising bed level.

However, it can be shown that a basic state with sloping banks (and non-zero sediment transport) does not exist within the same model and the new geometry. In earlier work, Parker [4] refers to this as the 'stable-channel paradox', as it contradicts observations in reality. It is an immediate consequence of the gravitational effect on the transport direction of sediment on side slopes. Parker notes that invoking secondary currents, actually excluded by the use of depth-averaged flow equations, is unlikely to resolve the paradox. This is because the corresponding lateral stresses are typically much smaller than the lateral erosive stress due to gravity. The paradox reveals a limitation of the frequently adopted physical model. An apparent weakness is the limited accuracy of the transport formula. This cannot be a surprise as a single formula is supposed to cover the complicated sediment physics within the river bed, more or less for sake of modelling closure. Apparently the mechanisms are not (yet) properly understood.

This shortcoming justifies the choice for an alternative approach, e.g. using a variational principle. This means that the dynamics is dropped, and all attention is paid to the basic state. Hence, the necessity of describing physical mechanisms in detail is circumvented.

Instead, an optimization principle should be adopted with respect to certain functionals. Hence, variational modelling provides an alternative way of studying rivers, without being too specific about the mechanisms that are not yet properly understood anyway. The limitation of the direct physical model is interpreted as giving some freedom in the variational modelling. In the present study this approach is adopted to study cross-sectional river profiles.

Variational principle

The cross-sectional shape of a river with erodible bed and banks can take up various shapes. One way to investigate these profiles is to adopt a varia-

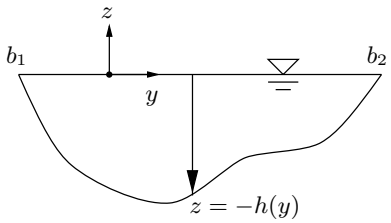

Figure 1: Definition sketch of the geometry.

tional approach. To that end, assume that a river uses a part of the energy expenditure to maintain its cross-sectional shape. From this point of view, the most interesting profile is the one for which this energy-like quantity is minimal. Lamberti [3] refers to this as the hypothesis of Minimum Energy Dissipation Rate (MEDR).

The total resistance or bed friction can serve as the quantity to be minimized. However, the minimization process only makes sense if it is carried out on the levelsets of a second functional, e.g. the water discharge of the river. Among other possibilities, the discharge is a reasonable constraint as it is closely related to the amount of water that has to find its way down the river. Hence the following constrained variational problem is proposed:

$$\min_h \{R(h) \;\mid\; Q(h) = q\}\,. \tag{1}$$

Here, R and Q are the resistance and discharge, respectively, formulated as functionals of the cross-sectional profile h. Let $h(y)$ denote the local depth of the river as a function of the transverse coordinate y ($b_1 \leq y \leq b_2$). See figure 1. Furthermore, it is realistic to include a second constraint in the present model. Requiring the lateral bed slope $h_y \equiv \frac{\partial h}{\partial y}$ to be bounded by a certain maximum, i.e.

$$|h_y| \leq \mu, \qquad \text{for all } b_1 \leq y \leq b_2, \tag{2}$$

reflects a fundamental property of noncohesive sediment. Here $\mu = \tan\phi$ is a material constant with ϕ representing the angle of repose of the sediment. In natural sediment this angle is found to take values typically between 30° and 40° (see Van Rijn [6]).

Summarizing, profiles of equal discharge are compared in order to find the one(s) with minimal resistance. Note that this approach is stationary and, therefore, the effects of temporal variations in e.g. water discharge cannot be included. Obviously, this approach requires specifying resistance and discharge functionals.

Resistance and discharge expressions

In this section expressions for the two functionals, i.e. the resistance and the discharge, will be derived.

Resistance

Firstly, an expression for the resistance will be derived. For the resistance one can write

$$R \equiv \tau_b P = \rho g i_0 A. \tag{3}$$

Here, τ_b is the average bed shear stress, averaged over the wetted perimeter P. The second equality is a straightforward force balance, stating that the total resistance equals the longitudinal component of the water weight. Here ρ is the water density, g the acceleration of gravity and i_0 the energy slope. By definition, the latter equals the longitudinal surface slope, which is assumed to be small. Finally A represents the cross-sectional area. The above indicates that this quantity is a suitable measure for the total flow resistance, i.e.

$$R(h) = \rho g i_0 A(h) = \rho g i_0 \int_{b_1}^{b_2} h \, dy. \tag{4}$$

Discharge

Now the expression for the discharge will be derived. Let U denote the cross-sectionally averaged longitudinal flow velocity. An expression for U will be derived from Chézy's theory, which can also be found in Chow [1] and Fowler [2]. The assumption of a turbulent flow allows the use of a friction law given by

$$\tau_b = f \rho \, U^{1/m}, \tag{5}$$

where f is a parameter. Since various friction relations exist, the exponent is described by introducing the parameter m. Fowler [2] suggests the range $\frac{3}{2} \leq \frac{1}{m} \leq 4$, which contains Chézy's choice $\frac{1}{m} = 2$, corresponding to a quadratic friction law.

Combining the above with the force balance in (3) yields a relationship linking the three quantities U, A and P

$$U = C i_0^m R_{\text{hyd}}^m, \tag{6}$$

with $C = (g/f)^m$ and $R_{\text{hyd}} \equiv A/P$ is called the hydraulic radius of the river profile. For $m = \frac{1}{2}$ it is known as Chézy's formula and C is called the Chézy coefficient. Multiplying (6) by A gives an expression for the water discharge:

$$Q = A\,U = C i_0^m \frac{A^{m+1}}{P^m}. \tag{7}$$

Formulated as a functional of the profile h this takes the following form:

$$Q(h) = C i_0^m \frac{\left(\int_{b_1}^{b_2} h\; dy\right)^{m+1}}{\left(\int_{b_1}^{b_2} \sqrt{1+h_y^2}\; dy\right)^m}. \tag{8}$$

Here it has been used that P is simply the arclength of the profile. The validity of the thus obtained expressions largely depends on the validity of equating τ_b in (3) and (5).

Properties of the optimal river shapes

Consider the variational problem (1) in which the functionals are given by (4) and (8):

$$\min_h \{R(h) \;\mid\; Q(h) = q, \quad |h_y| \le \mu\}. \tag{9}$$

Note that the bed slope restriction (2) has been included in this formulation.

In this section two properties of (9) will be shown: the shape of the optimal profile is independent of the value of the constraint q and the water domain of the optimizing profile $h = h_{\text{opt}}(y)$ is a convex set. Also some remarks on braided rivers will be made. It is stressed that these results can be stated before solving (9) explicitly, which will be carried out next.

Scaling argument

To prove that the shape of the optimal profile is independent of q, a scaling argument is invoked. Consider a family of similarly shaped profiles, being magnifications of one another, parametrized by a length scale ℓ, such as width or depth. Then $A = \alpha\ell^2$ and $P = \beta\ell$ define the nondimensional shape factors α and β which are constants within each family. As a result, $Q = C i_0^m \alpha^{m+1} \beta^{-m} \ell^{m+2}$ or, conversely, $\ell = (C^{-1} i_0^{-m} \alpha^{-(m+1)} \beta^m Q)^{1/(m+2)}$. Then from (7):

$$R = K\,\gamma^{\frac{m}{m+2}} Q^{\frac{2}{m+2}}, \tag{10}$$

in which $\gamma \equiv \beta^2/\alpha$ is a new shape factor and K a constant given by

$$K = \rho\, g\, C^{\frac{-2}{m+2}}\, i_0^{\frac{2-m}{m+2}}.$$

From (10) it is seen that solving (9), i.e. minimizing R for a fixed $Q = q$ can be done by minimizing the shape factor γ over all feasible families. Suppose this minimizing process has been carried out and has led to a minimum $\gamma_{\min}$, this $\gamma_{\min}$ characterizes the optimal family, to which all solutions of (9) belong: profiles of similar shape, only their size being related to the value of q. This completes the proof.

Two remarks are appropriate.

- The relation in the previous paragraph between the length scale ℓ, e.g. the maximal depth H and the discharge q, takes for Chézy's choice $m = \frac{1}{2}$ the following form:

  $$H \propto q^{2/5}.$$

  This relation was earlier obtained by Rorink-Heerink *et al.* [5] and was found to agree well with natural river data.

- Note that the definitions of α and β imply that the nondimensional ratio γ can also be written as

  $$\gamma = \frac{P^2}{A}. \tag{11}$$

  Apparently, the quantity to be minimized does not depend on m. Hence, the shape of the optimal profile will not depend on the choice for the exponent in the friction law (5).

Convexity of the optimal water domain

With the use of the previous results it can easily be shown that the optimal profile gives a convex water domain. Convexity means that any straight line connecting two points on the profile fully lies within the water domain, as depicted in figure 2(a). For rivers this is a natural property. Now suppose the optimal water domain is not convex, e.g. like in figure 2(b). Then two points p_1 and p_2 exist such that the profile is above the straight line connecting them. Define a new profile $\tilde{h}$ as a modification of h_{opt}, replacing the local violation of convexity with a straight line. It is immediately seen that $\tilde{A} > A$ and $\tilde{P} < P$, and so $\tilde{\gamma} = \tilde{P}^2/\tilde{A} < P^2/A = \gamma_{\min}$, which is a contradiction. This completes the proof.

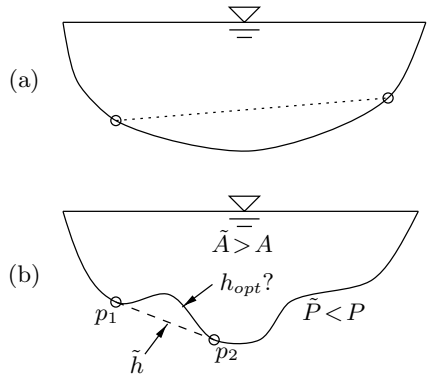

Figure 2: (a) Example of a profile with a convex water domain. (b) The optimal profile has this property, since replacing a supposed violation of convexity (between p_1 and p_2) with a straight line leads to a modified profile with a smaller perimeter, a larger area and, hence, a smaller γ.

Braided rivers

Evaluating (10) for the optimal profile h_{opt} will give the value function: by definition the minimal R as a function of the value of the constraint q:

$$R_{\min}(q) = K\, \gamma_{\min}^{\frac{m}{m+2}} q^{\frac{2}{m+2}}.$$

As $m > 0$, the value function is concave. Mathematically, this property is essential for the well-posedness of the variational problem. It guarantees that splitting a river into two or more smaller ones, together carrying the same discharge, is less favourable as it will always increase the total friction.

For example, take Chézy's choice $m = \frac{1}{2}$ and compare two situations: one big river carrying discharge q versus two smaller rivers, each carrying $\frac{1}{2}q$. See figure 3. For the total friction ratio, it is found that

$$\frac{R_{\min}^{\text{two}}(q)}{R_{\min}(q)} = \frac{2R_{\min}(\frac{1}{2}q)}{R_{\min}(q)} = 2^{1/5} \approx 1.15.$$

Apparently, this particular way of splitting the river is attended with a 15 percent increase in total friction. Such a braided river with several parallel streams will be found as a local minimizer.

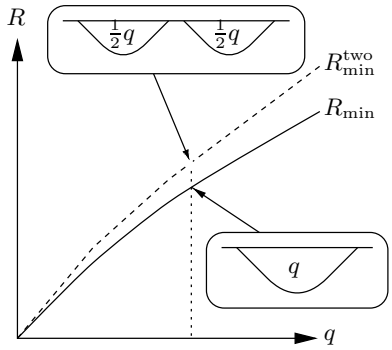

Figure 3: Splitting one big river of discharge q into two smaller ones, each of discharge $\frac{1}{2}q$. The plots show that, for a given q, the latter situation has a larger total friction: $R_{\min}^{\text{two}} > R_{\min}$.

Optimal river shapes

The previous section has shown that the variational problem (9) can be solved in two steps. Firstly, minimize the shape factor γ, given by (11):

$$\min_h \left\{ \gamma \equiv \frac{P(h)^2}{A(h)} \;\; | \;\; |h_y| \leq \mu \right\} \tag{12}$$

This leads to an optimal *family* of similarly shaped profiles and a value of $\gamma_{\min}$. Secondly, from this family, pick the *profile* with the right size, i.e. the one that satisfies the discharge constraint $Q(h) = q$. The present subsection deals with the first step (the second step being rather straightforward): solving the variational problem (12). Of particular interest is the dependence of the results on the parameter μ $(= \tan\phi)$.

Without slope restriction

Firstly, the case $\mu = \infty$ $(\phi = 90°)$ will be addressed, which is equivalent to switching off the slope constraint. Solving this type of variational problems generally leads to a differential equation for the optimizing function. In the present case, it is a second order differential equation, which, after integrating once, takes the following form:

$$\frac{h_y}{\sqrt{1+h_y^2}} = \frac{y_0 - y}{r}. \tag{13}$$

The positive constant r is the scale parameter of the family, later to be related to the value of the constraint q. Furthermore, y_0 is a constant of integration, determining the point where the profile is horizontal, i.e. where $h_y = 0$. With the choice $y_0 = 0$ the solution $h = h(y)$ is given by:

$$(h + h_0)^2 + y^2 = r^2, \tag{14}$$

where h_0 is an integration constant. This corresponds to a circular profile with the circle center at a height h_0 above the water level. See figure 4(a). The choice for h_0 that minimizes γ turns out to be $h_0 = 0$. Hence, the water level of the optimal profile passes exactly through the circle center, as depicted in figure 4(b). This profile will be referred to as a halfpipe. The corresponding value of the shape factor is $\gamma = 2\pi$.

The optimal profile being a circle cannot be considered a surprise by realizing that *minimizing* A for a given $A^{3/2}P^{-1/2}$ is equivalent to *maximizing* A for a given P. This classical problem is called Dido's problem [8], the solution of which is known to be a (closed) circle. Its equivalent in case of river profiles is obviously one half of the circle, i.e. the halfpipe.

With slope restriction

A halfpipe, however, due to its vertical banks, is not feasible if the slope restriction (2) is incorporated: $\mu < \infty$ ($\phi < 90°$). The optimal profile will be different. It contains parts of two types. (i) Parts where the slope constraint (2) is not active. Here, the differential equation (13) is valid, leading to circular shapes as seen from (14). (ii) Parts where the slope constraint is active: $|h_y| = \mu$. This obviously leads to straight lines of slope $\pm\mu$.

Constructing the profile from parts of these two types inevitably leads to the shape depicted in figure 4(c): a circular part in the middle, whose endpoints a_1 and a_2 are connected to the banks by straight lines. From variational theory it is known that the parts connect smoothly (slope continuously). This determines the exact location of a_1 and a_2, i.e. where the circular part has slope $\pm\mu$.

One degree of freedom still exists: the optimal surface level. Like in the case without slope restriction, it turns out that the optimal surface level passes exactly through the circle center. See figure 4(d). The corresponding value of the shape factor, expressed in terms of the parameter ϕ, is found to be

$$\gamma_{\phi,\min} = 4(\phi + \cot\phi), \tag{15}$$

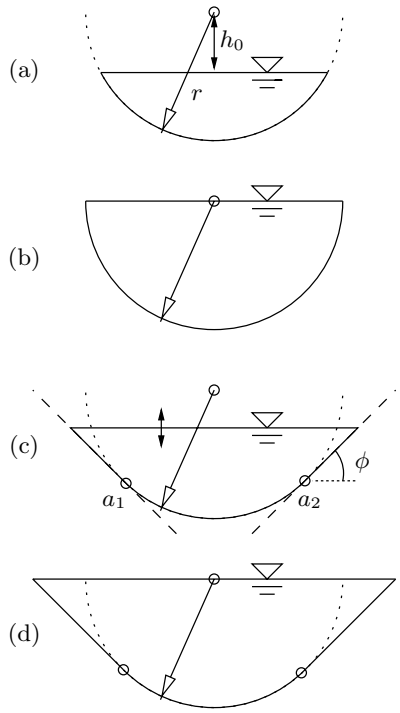

Figure 4: (a) Circular profile (14) of radius r and interpretation of integration constant h_0. (b) The optimal profile is a halfpipe, i.e. a circular profile with $h_0 = 0$. (c) profile constructed from circular and linear parts, with connection points a_1 and a_2. (d) the water level of the optimal profile passes exactly through the circle center.

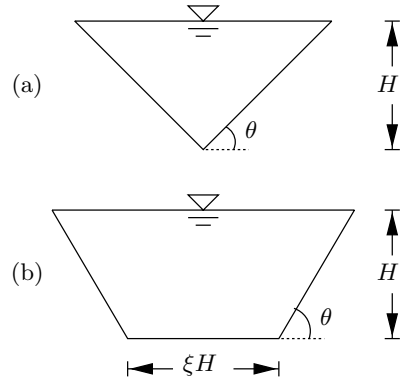

Figure 5: Basic channel shapes with kinks: (a) V-gully, (b) trapezoidal channel.

(note: ϕ in radians). For $\phi = \pi/2$, i.e. after dropping the slope constraint, the previously obtained $\gamma_{\min} = 2\pi$ of the halfpipe is recovered.

Finally, it is noted that the width to depth ratio of the optimal profile depends on the angle of repose according to

$$\frac{B}{H} = \frac{2}{\sin\phi}.$$

This aspect ratio roughly takes values between 3 and 4 for values of the angle of repose between 30° and 40°.

Comparison with basic channel shapes

The techniques used in the previous subsection ignore profiles containing slope discontinuities. Indeed, the optimal profile does not feature any of these kinks. However, one can easily think of some profiles that do contain kinks. The present subsection is devoted to a comparison between the optimal profile and two of these basic channel shapes: the V-gully and the trapezoid. See figure 5. Criterion of comparison will be the value of the shape factor γ, given by (11). Again, the dependence on the angle of repose ϕ is of particular interest.

Consider a V-gully of bank angle $\theta \leq \phi$ and depth H, as depicted in figure 5(a). For the value of $\gamma = P^2/A$ one finds

$$\gamma^{\text{Vgully}}(\theta) = \frac{8}{\sin 2\theta},$$

of course not depending on H. This function has a global minimum of 8 at $\theta = 45°$. Hence, choose $\theta = 45°$ whenever permitted by the constraint and otherwise take $\theta = \phi$, i.e. the steepest possible bank slope. This leads to

$$\gamma_\phi^{\text{Vgully}} = \begin{cases} \frac{8}{\sin 2\phi}, & \phi \leq 45° \\ 8, & \phi > 45°. \end{cases} \tag{16}$$

Next, consider the trapezoidal channel of bank angle $\theta \leq \phi$ and with a horizontal bed part of length ξH with H the depth, as depicted in figure 5(b). Note that for $\xi = 0$ the trapezium channel reduces to the V-gully. The value of the shape factor can be expressed in terms of θ and ξ according to

$$\gamma^{\text{trap}}(\theta, \xi) = \frac{\left(\xi + \frac{2}{\sin\theta}\right)^2}{\xi + \cot\theta}.$$

Minimizing γ^{trap} first for fixed θ and variable ξ gives an optimal value $\xi_{\text{opt}} = 2(1 - \cos\theta)/\sin\theta$. The corresponding value of γ reads

$$\gamma^{\text{trap}}(\theta) = 4\frac{2 - \cos\theta}{\sin\theta}.$$

This function has a global minimum of $4\sqrt{3}$ at $\phi = 60°$. Analogously to the above, one finds

$$\gamma_\phi^{\text{trap}} = \begin{cases} 4\frac{2-\cos\phi}{\sin\phi}, & \phi \leq 60°, \\ 4\sqrt{3}, & \phi > 60°. \end{cases} \tag{17}$$

The three γ-curves (15), (16) and (17) are plotted in figure 6. It is readily seen that, especially for larger values of ϕ, the extended halfpipe is more favourable than the others. Moreover, the observation that the V-gully is a special case of the trapezoidal channel explains why the latter behaves better. Finally, for small ϕ the curves show the same behaviour, as the three profiles effectively become similar.

Discussion

The variational principle adopted in the present study is to minimize total bed friction for a given discharge. This approach has led to cross-sectional river profiles with the following properties: its shape does not depend on the discharge constraint $Q(h) = q$ and not on the specific choice for the exponent in the friction law (5), but does depend on the angle of repose ϕ.

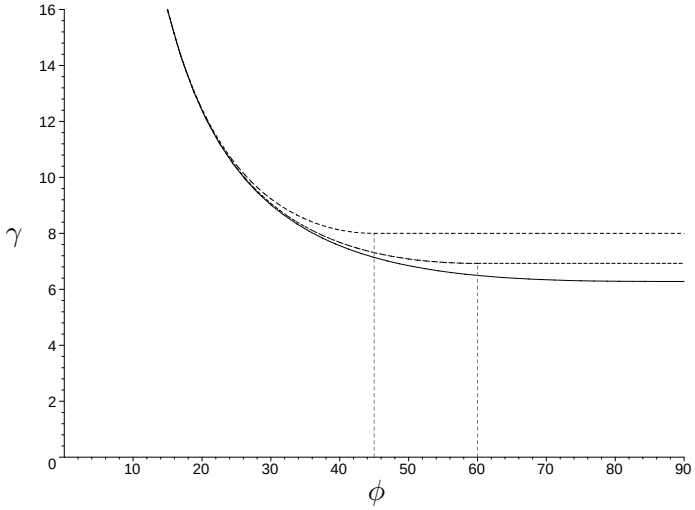

Figure 6: Dependence of the shape factor γ_ϕ on the angle of repose ϕ for various profiles: V-gully (dotted line), trapezoidal channel (dashed line) and extended halfpipe (solid line).

Besides these results, two important properties or features of the model can be identified: (i) it is based on a global rather than local relation and (ii) it is stationary. The implications of these will be discussed below.

(i) The global character of Chézy's formula (6) indicates that no detailed information is available on the interaction between water and bed. Nevertheless, there are various theoretical techniques to obtain a local functional, i.e. an expression written as a single integral. The most straightforward way to do this is to choose a particular partitioning in subchannels and to apply Chézy's theory to each of these subchannels. Summing all contributions now gives rise to an alternative discharge functional (the friction functional (4), in fact already a local expression, is unaffected):

$$Q_{\mathrm{loc}}(h) = C i_0^m \int_{b_1}^{b_2} \frac{h^{m+1}}{\left(1+h_y^2\right)^{m/2}} dy.$$

Observe the similarities with (8). It can be shown that using $Q_{\mathrm{loc}}(h)$ instead of $Q(h)$ does not alter the optimal profile significantly, provided the angle of repose does not exceed the typical values observed in natural sediment ($\phi \leq 40°$).

(ii) A second important feature of the model is its stationarity. Although

it states that nature has a preference for the obtained optimal profiles, this does not imply that these are the only shapes to be observed in nature. In order to investigate this, the actual evolution of river shapes comes into play and dynamics must be included in the model. In such dynamical processes suboptimal profiles might play a vital role, as an example of which braided rivers were mentioned.

References

[1] Chow, V.T., *Open channel hydraulics,* McGraw-Hill, Auckland etc., 1959.

[2] Fowler, A.C., *Mathematical models in the applied sciences*, Cambridge University Press, Cambridge, 1997.

[3] Lamberti, A., 'Dynamic and variational approaches in the river regime relation', in *Entropy and energy dissipation in water resources*, edited by V.P. Singh and M. Fiorentino, pp. 507-525, Kluwer Academic Publishers, 1992.

[4] Parker, G., 'Self-formed straight rivers with equilibrium banks and mobile bed. Part 2. The gravel river', *J. Fluid Mech., 89*, 127-146, 1978.

[5] Rorink-Heerink, H.M.J., E. Van Groesen and H.J. de Vriend, 'On stable alluvial channels: a variational approach', in *Environmental and coastal hydraulics: protecting the aquatic habitat*, vol. 2, pp. 1008-1013, ASCE, 1997.

[6] Rijn, L. C. van, *Principles of sediment transport in rivers, estuaries and coastal seas,* Aqua Publications, Amsterdam, 1993.

[7] Schielen, R., A. Doelman and H.E. de Swart, 'On the nonlinear dynamics of free bars in straight channels', *J. Fluid Mech., 252*, 325-356, 1993.

[8] Tikhomirov, V.M., *Stories about Maxima and Minima,* Mathematical World Volume 1, American Mathematical Society, 1986.

Appendix: Local Chézy

Discharge as a density functional

Observe that Chézy's formula (6) relates integrated quantities such as A, P and U rather than local quantities. In the following it is shown how to derive

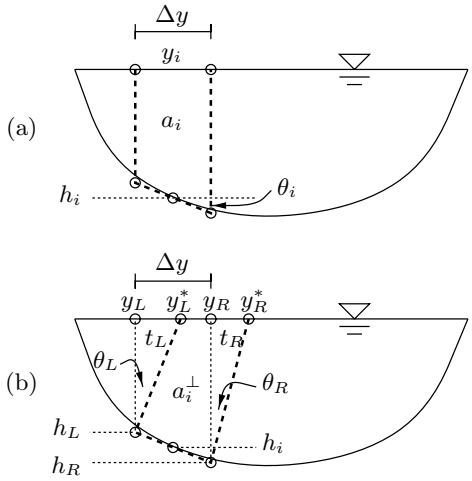

Figure 7: Partitioning the river in (a) linearly sloping subchannels with vertical banks and (b) linearly sloping subchannels bounded by bed normals.

a expression for the discharge that is a density functional, i.e. based on a local relationship. To that end, consider the profile as a union of adjacent linearly sloping channels of average depth h_i, width Δy and with a slope angle of θ_i. See figure 7(a). For such an elementary subchannel one finds that its area a_i, perimeter p_i and hydraulic radius $r_{\mathrm{hyd},i}$ are given by

$$a_i = h_i \Delta y, \quad p_i = \underbrace{2h_i}_{\text{banks}} + \underbrace{\frac{\Delta y}{\cos\theta_i}}_{\text{bed}}, \quad r_{\mathrm{hyd},i} = \frac{a_i}{p_i}, \tag{18}$$

respectively. Neglecting the contributions of the fictitious vertical banks to the perimeter, causes the hydraulic radius to collapse into

$$r_{\mathrm{hyd},i} = h_i \cos\theta_i. \tag{19}$$

Applying (8) to each of the elementary channels yields

$$q_i = C i_0^m \; h_i^{m+1} \cos^m \theta_i \; \Delta y. \tag{20}$$

Summing (20) over all subchannels gives an expression for the total discharge of the river. After letting $\Delta y \downarrow 0$ and with the use of $\tan\theta = h_y$, an alternative discharge functional is obtained:

$$Q_{\mathrm{loc}}(h) = C i_0^m \int_{b_1}^{b_2} \frac{h^{m+1}}{\left(1 + h_y^2\right)^{m/2}} dy. \tag{21}$$

Observe the way in which the slope term in (20) appears in the denominator of the integrand in (21).

Alternative density functional

The previous subsection discussed a particular partitioning: using subchannels with vertical banks. This suggests that a piece of river bed only 'feels' the water in the vertical above it. Especially at relatively large bed slopes, this might be questionable. An alternative would be to state that the actual interaction is between the bed element and water column *normal* to it. This approach suggests a partitioning in subchannels bounded by normals to the bed. See figure 7(b).

The derivation is somewhat more cumbersome. Consider the subchannel around $y = y_i$ between y_L and y_R ($\Delta y \equiv y_R - y_L$), consisting of straight lines only. The bed part has a slope $\tan\theta_i \equiv h_y(y_i)$ and the heights at the endpoints of the bed parts are h_L and h_R. The corners at the water surface are at y_L^* and y_R^*. Moreover, the fictitious banks are normal to the *local* bed slope angles θ_L and θ_R. As a result, it is found that

$$y_L - y_L^* = h_L \tan\theta_L, \quad y_R - y_R^* = h_R \tan\theta_R. \tag{22}$$

Now, the subchannel area $a_i^\perp$ is given by

$$a_i^\perp = a_i + t_R - t_L, \tag{23}$$

with a_i as in (18) and t_L and t_R representing two triangle areas. It is easily seen that

$$t_L = \frac{1}{2} h_L (y_L - y_L^*) = \frac{1}{2} h_L^2 \tan\theta_L, \tag{24}$$

and similarly for t_R. This gives the following expression for the subchannel area:

$$a_i^\perp = h_i \Delta y + \frac{1}{2}\left(h_R^2 \tan\theta_R - h_L^2 \tan\theta_L\right), \tag{25}$$

and the perimeter $p_i^\perp$ is found to be

$$p_i^\perp = \underbrace{\frac{h_L}{\cos\theta_L} + \frac{h_R}{\cos\theta_R}}_{\text{banks}} + \underbrace{\frac{\Delta y}{\cos\theta_i}}_{\text{bed}}. \tag{26}$$

Neglecting the contributions of the fictitious banks causes the hydraulic radius $r^{\perp}_{\mathrm{hyd},i}$ to collapse into

$$r^{\perp}_{\mathrm{hyd},i} = \cos\theta_i \left(h_i + \frac{h_R^2 \tan\theta_R - h_L^2 \tan\theta_L}{2\Delta y} \right) \tag{27}$$

Applying (8) now yields:

$$q_i^{\perp} = C i_0^m \left(h_i + \frac{1}{2} \left(h_R^2 \tan\theta_R - h_L^2 \tan\theta_L \right) \right)^{m+1} \cos^m \theta_i \Delta y \tag{28}$$

An expression for the total discharge is found by summing over all subchannels. After taking the limit $\Delta \downarrow 0$ this yields the functional:

$$Q^{\perp}_{\mathrm{loc}}(h) = C i_0^m \int_{b_1}^{b_2} \frac{\left(h + \frac{1}{2} \left(h^2 h_y \right)_y \right)^{m+1}}{\left(1 + h_y^2 \right)^{m/2}} dy \tag{29}$$

It is seen that curvature terms appear in the numerator of the integrand.

Note that (29) can also be written as

$$Q^{\perp}_{\mathrm{loc}}(h) = C i_0^m \int_{b_1}^{b_2} \frac{h^{m+1}}{\left(1 + h_y^2 \right)^{m/2}} \underbrace{\left(1 + h_y + \frac{1}{2} h\, h_{yy} \right)^{m+1}}_{\text{curvature}} dy, \tag{30}$$

where the extra curvature terms are written as a factor in the integrand.

The derivation above only holds when all subchannels look like the one depicted in figure 7. Problems arise if the two bed normals would intersect below the water level. This can be prevented by requiring $y_R^* \geq y_L^*$. This can be translated into a curvature condition for the profile, given by

$$\left(h\, h_y \right)_y \geq -1. \tag{31}$$

Hence, the functional (29) is only valid for profiles that satisfy this curvature condition. In case of rivers, this condition is acceptable as it does not exclude interesting profiles. For example, the halfpipe satisfies (31) with equality everywhere, as all normals intersect in the circle center.

Differential equation

This section is devoted to solving the variational problem if the density discharge functional $Q_{\mathrm{loc}}(h)$ is taken instead of $Q(h)$. Therefore, consider (1) with the functionals given by (3) and (21):

$$\min_h \left\{ R(h) \;\middle|\; Q_{\mathrm{loc}}(h) = q, \quad |h_y| \leq \mu \right\}. \tag{32}$$

The slope restriction (2) has been included in this formulation. Euler-Lagrange theory shows that the constrained variational problem (32) can be rewritten into an unconstrained one, according to

$$\min_h \{L(h) \equiv A(h) - \lambda Q_{\text{loc}}(h)\}. \tag{33}$$

Here λ is Lagrange's multiplier, a constant depending on the value of the constraint q. Minimizing a functional $L(h, h_y) = \int \ell(h, h_y)dy$ in which the integrand $\ell(h, h_y)$ does not depend explicitly on y, a principle of conserved energy holds:

$$h_y \frac{\partial \ell}{\partial h_y} - \ell(h, h_y) = E \tag{34}$$

in which E is a constant. Evaluating this for the integral L, yields

$$h^{m+1} \frac{1 + (m+1)h_y^2}{(1 + h_y^2)^{m/2+1}} - \frac{h}{\lambda} = E. \tag{35}$$

Here, λ represents Lagrange's multiplier E is a constant for which $E = 0$ is taken. Furthermore, one can expect the bottom to be horizontal in the deepest part of the river. Inserting $h_y = 0$ into (35) now yields $\lambda = h_0^{-m}$ with h_0 representing this maximal depth. Using these results, one can rewrite (35) into

$$\frac{h}{h_0} = \frac{(1 + h_y^2)^{\frac{1}{m}+\frac{1}{2}}}{(1 + (m+1)h_y^2)^{1/m}}. \tag{36}$$

Figure 8 shows a plot of the relation between h/h_0 and h_y according to (36), for Chézy's choice $m = \frac{1}{2}$. The plot has a global minimum of 0.8965 at $h_y^2 = \frac{2}{3}$ (which corresponds to a transverse bed slope angle $\beta = 39°$). This means that (36) only provides information in the deepest part of the river where $0.8965 \leq h/h_0 \leq 1$. It is therefore unclear how the optimal profile looks in the shallower part of the river.

For non fixed m, the minimum is attained at $h_y^2 = \frac{1}{m+1}$. The corresponding angle, actually the largest possible angle from the differential equation, is plotted against m in figure 9.

The solution of (36), obtained numerically for $m = \frac{1}{2}$, is plotted in figure 10.

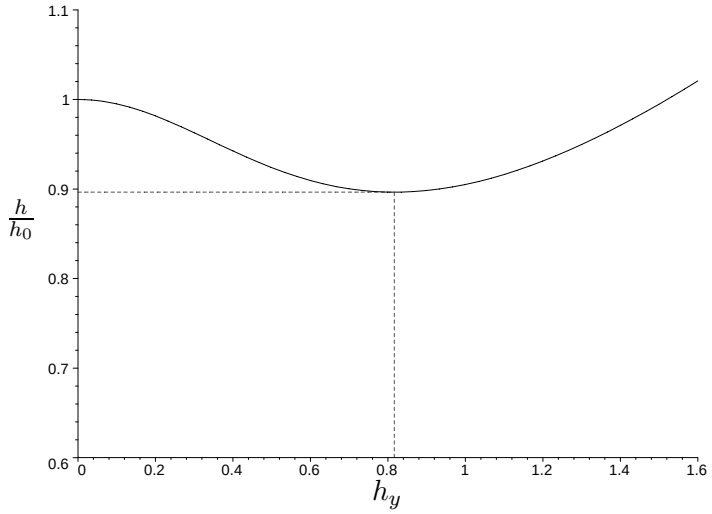

Figure 8: h/h_0 versus h_y according to the differential equation (36). Note: $m = \frac{1}{2}$.

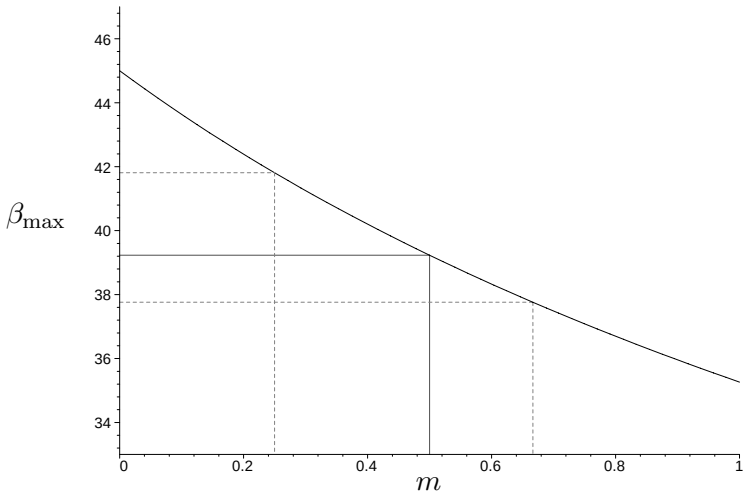

Figure 9: Dependence of the maximal angle on m, as derived from (36).

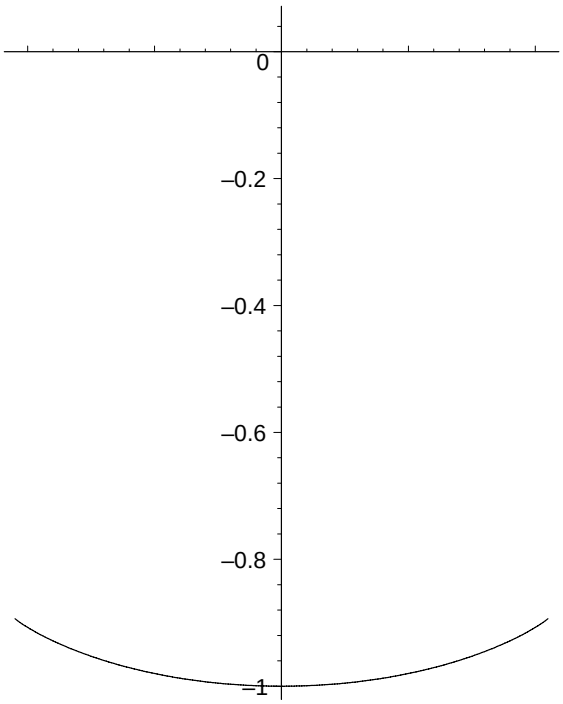

Figure 10: Numerical solution of (36). Note: $m = \frac{1}{2}$.

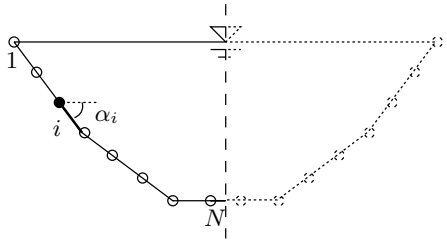

Figure 11: Definition sketch of the chain approach.

Numerical chain approach

An alternative approach to the variational problem (32) can be obtained by focusing on the value function. Analogously to the derivation in the previous section, it follows that a relation of the form (10) holds. The constant γ is now given by the nondimensional ratio

$$\gamma = \frac{A^{1+2/m}}{Q_{\text{dens}}^{2/m}}, \tag{37}$$

which should be minimal for the optimal profile. This provides an alternative criterion for optimality, which, due to its size-invariance, allows the problem to be investigated with an extra degree of freedom. In the following this will be carried out numerically.

Consider the part of the river profile from one of its banks to its deepest part[2]. This part of the profile can be approximated by a chain of N nodes and N straight lines of equal length. See figure 11. At each node i, an angle α_i is defined to represent the angle of the corresponding line with the horizontal. Hence, the river profile can be characterized by the values of α_i for $i = 1, \ldots, N$, as a function of which the corresponding value of γ can be calculated:

$$\gamma = \gamma(\alpha_1, \alpha_2, \ldots, \alpha_N). \tag{38}$$

Given a certain initial profile, it is obvious that the angles α_i might be modified such that γ decreases. Proceeding systematically, this procedure is likely to yield both a minimal value of γ and an optimal profile. Note that

[2]It is sufficient to consider one half since one can easily prove that the optimal profile will be symmetric.

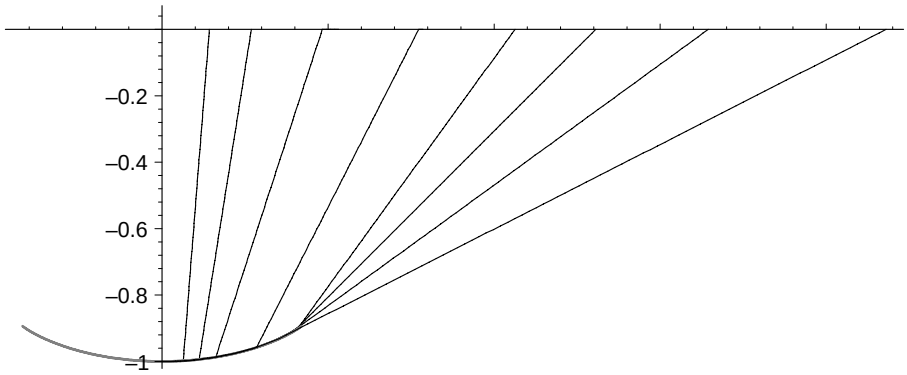

Figure 12: Optimal profile obtained numerically using the chain approach. Calculated for various values of the angle of repose (from right to left): $\phi = 27°$, $36°$, $45°$, $54°$, $63°$, $72°$, $81°$ and $85.5°$. The solution of (36) is plotted as well. The plots are made nondimensional with the maximal depth h_0.

the slope restriction (2) can easily be incorporated by accepting the angle of repose as an upper bound for each α_i:

$$\alpha_i \leq \phi, \qquad \text{for } i = 1, \ldots, N. \tag{39}$$

Three remarks are appropriate.

- There is no guarantee that the obtained local minimum is a global minimum as well. Hence, the choice of the initial profile might be important.
- During the numerical process, the perimeter is kept at an arbitrary but fixed value, whereas both A and Q_{dens} change. This is the degree of freedom mentioned above, resulting from the size-invariance of γ.
- The chain approach implies an equidistant discretization of the wetted perimeter instead of the transverse coordinate y. This is done because the latter method cannot handle vertical bed slopes in a proper way.

The shape of the optimal profile, for various values of ϕ is plotted in figure 12. One can clearly distinguish between a bed part in the channel center and a bank part. The bed part matches the numerical solution of (36) quite well. The banks are straight and their slope corresponds to the angle of repose. Finally, observe that the transition point between bed and banks shifts towards the center for increasing ϕ.